NASA Technical Memorandum 103681

Computational Simulation of Hot Composites Structures

C.C. Chamis and P.L.N. Murthy
National Aeronautics and Space Administration
Lewis Research Center
Cleveland, Ohio

S.N. Singhal
Sverdrup Technology, Inc.
Lewis Research Center Group
Brook Park, Ohio

Prepared for the
Energy-Sources Technology Conference and Exhibition
sponsored by the American Society of Mechanical Engineers
Houston, Texas, January 20–24, 1991

COMPUTATIONAL SIMULATION OF HOT COMPOSITES STRUCTURES

C.C. Chamis,* and P.L.N. Murthy,**
National Aeronautics and Space Administration
Lewis Research Center
Cleveland, Ohio 44135

S.N. Singhal***
Sverdrup Technology, Inc.
Lewis Research Center
Brook Park, Ohio 44142

SUMMARY

Three different computer codes developed in-house are described for application to hot composite structures. These codes include capabilities for: (1) laminate behavior (METCAN), (2) thermal/structural analysis of hot structures made from high temperature metal matrix composites (HITCAN), and (3) laminate tailoring (MMLT). Results for select sample cases are described to demonstrate the versatility as well as the application of these codes to specific situations. The sample case results show that METCAN can be used to simulate cyclic life in high temperature metal matrix composites; HITCAN can be used to evaluate the structural performance of curved panels as well as respective sensitivities of various nonlinearities; and MMLT can be used to tailor the fabrication process in order to reduce residual stresses in the matrix upon cool-down.

INTRODUCTION

High temperature metal matrix composites (HT-MMCs) are emerging as materials with potentially high payoffs in aerospace structural applications. Realization of these payoffs depends on the parallel and synergistic development of: (1) a technology base for fabricating HT-MMC structural components, (2) experimental techniques for measuring their thermal and mechanical characteristics, and (3) computational methodologies for predicting their nonlinear behavior in complex service environments. In fact, it might be argued that the development of computational methodologies should precede the others because the structural integrity and durability of HT-MMCs can be computationally simulated, and the potential payoff for a specific application can be assessed, at least qualitatively. In this way, it is possible to minimize the costly and time consuming experimental effort that would otherwise be required in the absence of a predictive capability.

Recent research at NASA Lewis is directed towards the development of a computational capability to predict the nonlinear behavior of HT-MMCs. This capability is in the form of stand-alone computer codes which are used to computationally simulate HT-MMC behavior in all its inherent scales. The simulation starts with constituents and the fabrication process and proceeds to determine the effects induced by the severe service loading environments. Three computer codes have been

---

*Senior Aerospace Scientist, Structures Division.

**Senior Aerospace Engineer, Structures Division.

***Senior Research Engineer.

developed to-date: (1) METCAN - Metal-Matrix Composite Analyzer, (2) HITCAN - High Temperature Composite Analyzer, and (3) MMLT - Metal Matrix Laminate Tailoring. These codes were developed in the order mentioned above. The amount of discussion allotted for each code reflects directly the experience we had with each code. Each of these codes simulates a specific area of HT-MMCs. For example: (1) METCAN is structured to simulate HT-MMCs behavior at a point, (2) HITCAN is developed to analyze the behavior of hot structures with active cooling provisions (passages) made from HT-MMCs, and (3) MMLT is developed to concurrently tailor the constituent materials characteristics and the fabrication process for an a priori specified HT-MMC behavior such as minimum residual stresses upon cool-down. The primary objective of this article is to briefly describe these three computer codes and present illustrative results from their applications to simulate specific HT-MMC behavior. The secondary objective is to demonstrate what can be done with these three computer codes but not how it is done. Select references are cited for that purpose.

METCAN - METAL MATRIX COMPOSITE ANALYZER

The structure of METCAN, its simulation capabilities, and typical results to illustrate the applications of these capabilities, are summarized in this section.

The structure of METCAN parallels the fabrication process of matrix composites. A typical fabrication process is schematically illustrated in figure 1. The simulation capability in METCAN is depicted schematically in figure 2. METCAN has the capability to predict all aspects of HT-MMC behavior, including the fabrication process by using only room temperature properties for the fiber and matrix. The formalism embedded in it, an initial version, and concept demonstration are described in reference 1. A detailed description of the micromechanics to repreresent the simulation at the constituent materials level is provided in reference 2.

Fundamental to the computational simulation in METCAN is the introduction of the multifactor interaction model (MFIM) to represent the various nonlinearities and their mutual interactions in the constituents. The equation form of the MFIM and reasons for its selection are summarized in figure 3. A discussion on its ability to represent constituent material behavior and the subsequent influence of this behavior on the response of structural components from HT-MMC is presented in reference 3.

The use of METCAN to simulate metal matrix composite behavior from consitutent material properties at room temperature is summarized in table I. Comparisons of these properties with three-dimensional finite elements are shown in table II (ref. 4). METCAN simulation of the cyclic behavior of HT-MMCs is described in reference 4, where the influence of the interphase and limited comparisons with room temperature data are also described. Illustrative results from reference 4 are shown in figure 4. It can be observed in this figure that cyclic loading influences the MMC stress/strain behavior and degrades the stress at fracture. METCAN simulation of in-situ behavior and how this can be used to interpret composite-measured behavior are described in reference 5. Results from reference 5 on the effects of in-situ matrix strength on unidirectional MMC transverse tensile and shear strengths are shown in figures 5(a) and (b), respectively. Degradation of in-situ matrix strength, compared to its bulk state, substantially degrades matrix dominated strengths. The degradation is severest for the transverse tensile strength. The degradation for longitudinal tension is negligible but it is considerable for longitudinal compression. Therefore, transverse tensile tests will be the most sensitive to experimentally detect any degradation.

Corresponding results for the development of an interphase between fiber and matrix, or weakening of the interfacial bond, are shown in figures 6(a) and (b) for transverse tensile and shear strengths, respectively. The interphase properties or the interfacial bond strength were assumed to be ratios of the matrix undegraded strength, while the in-situ matrix was assumed to retain its bulk state properties. It can be seen in figure 6 that the interphase degrades the stresses at fracture but does not degrade the stress/strain curve. There are other conditions of the in-situ matrix which can influence matrix strength as well. Some of these are shown in figure 7 (ref. 4). The annealed yield with no interfacial bond corresponds to very low values measured for these composites. In this context, METCAN can also be used to interpret measured data.

METCAN simulation of life under thermal cycles is shown in figure 8, where available measured data (ref. 6) is also shown for comparison. This very good comparison is considered adequate to demonstrate the simulation capability of METCAN for cyclic life.

HITCAN - HIGH TEMPERATURE COMPOSITE ANALYZER

HITCAN combines METCAN with a noncommercial finite element code, MHOST, and a dedicated mesh generator. The code is stand-alone and stream-lined for the thermal/structural analysis of hot metal matrix composite structures. A schematic of the code's structure is shown in figure 9, with its capabilities summarized in table III. An extensive description of HITCAN, including a variety of sample cases to illustrate its computational capabilities, are found in reference 7. The results for a curved panel are included herein as specific examples.

The panel geometry, laminate lay-up, and loading conditions (thermal, mechanical) are shown in figure 10. The buckling evaluation results are shown in figure 11. The buckling load decreases with fiber degradation (fiber diffusion into the matrix) and with temperature (material degrades due to temperature). The decrease, due to temperature, is substantial (about 30 percent). The panel vibration frequencies, displacement, ply and constituent stresses are summarized in figure 12. This figure illustrates the versatility (breadth and depth) of HITCAN to simulate MMC structural behavior and evaluate their adequacy in hot structures applications. HITCAN can also be used to perform sensitivity analyses. Results from sensitivity analyses for the curved panel are shown in figure 13.

Collectively, the results summarized demonstrate that the complex behavior of MMC structures can be simulated at all its scales by using an integrated computer code such as HITCAN.

MMLT - METAL MATRIX LAMINATE TAILORING

The Metal Matrix Laminate Tailoring computer code consists of METCAN with a suitable optimizer. This code has been recently initiated and only preliminary results have been obtained to date. The code is described in detail in reference 8. Herein, representative results are included to illustrate its application. The results are for a graphite fiber/copper-matrix composite where the fabrication process (temperature and consolidation pressure) histories are tailored to minimize the residual stresses in the matrix during cool-down from consolidation to room temperature. Constraints (conditions) were imposed in the tailoring procedure that

the residual stresses will not exceed the corresponding matrix strength during cool-down.

The tailored fabrication process is shown in figure 14. The microstress developed in the different matrix regions (A, B, or C, fig. 3) are shown in figure 15. These results demonstrate that MMLT can be used to process HT-MMCs for desired matrix stress magnitudes during the cool-down process as well as the sensitivities of the various parameters that influence the optimum fabrication process. For example, in the present study, the consolidation pressure history appeared to be one of the more important parameters that influence the optimum fabrication process.

CONCLUSIONS

Three computer codes have been developed and are described which can be used to simulate the complex behavior of hot structures made from high temperature metal matrix composites (HT-MMCs). These codes are: (1) Metal Matrix Composite Analyzer (METCAN), (2) High-Temperature Composite Analyzer (HITCAN), and (3) Metal Matrix Laminate Tailoring (MMLT). Results from each code for select sample cases are included to illustrate the capabilities of each code. The results from METCAN are for laminate properties, in-situ strength, interphase effects, and cyclic load effects. The results from HITCAN are for a curved panel subjected to thermal and mechanical loads and including various nonlinearities. HITCAN results for sensitivity analyses are also included. The results for MMLT are for tailoring the fabrication process in order to minimize the residual stresses in the matrix during cool-down. Collectively, the results from these sample cases demonstrate that computer codes can be developed to computationally simulate composite hot structure at all its scale levels.

REFERENCES

1. Hopkins, D.A., 1984, "Nonlinear Analysis of High-Temperature Multilayered Fiber Composite Structures - Turbine Blades," NASA TM-83754.

2. Hopkins, D.A. and Chamis, C.C., 1985, "A Unique Set of Micromechanics Equations for High Temperature Metal Matrix Composites," NASA TM-87154.

3. Chamis, C.C. and Hopkins, D.A., 1985, "Thermoviscoplastic Nonlinear Constitutive Relationships for Structural Analysis of High Temperature Metal Matrix Composites," NASA TM-87291.

4. Chamis, C.C., Murthy, P.L.N., and Hopkins, C.A., 1988, "Computational Simulation of High Temperature Metal Matrix Composites Cyclic Behavior," NASA TM-102115.

5. Murthy, P.L.N., Hopkins, D.A., and Chamis, C.C., 1989, "Metal Matrix Composite Micromechanics: In-situ Behavior Influence on Composite Properties," NASA TM-102302,

6. Chamis, C.C., Caruso, J.J., Lee, H.J., and Murthy, P.L.N., 1990, "METCAN Verification Status," NASA TM-103119.

7. Singhal, S.N., Lackney, J.J., Chamis, C.C. and Murthy, P.L.N., 1990, "Demonstration of Capabilities of High Temperature Composite Analyzer Code HITCAN," NASA TM-102560.

8. Saravanos, D.A., Murthy, P.L.N., and Morel, M., 1990, "Optimal Fabrication Process for Unidirectional Metal Matrix Composites: A Computational Simulation," NASA TM-102559.

TABLE I. - NOMINAL CONSTITUENT PROPERTIES AND PREDICTED COMPOSITE PROPERTIES AT ROOM TEMPERATURE

(a) SiC fiber

Fiber density, ρ_f, lb/in.^{3}	0.11
Fiber elastic modulus, E_f, Mpsi	62
Fiber Poisson's ratio, υ_f, in./in.	0.3
Fiber shear modulus, G_f, Mpsi	23.8
Fiber coefficient of thermal expansion, α_f, ppm	1.8
Fiber melting temperature, T_{Mf}, °F	4870
Fiber tension strength in direction 11, S_{f11T}, ksi	500
Fiber composite strength in direction 11, S_{f11c}, ksi	650
Fiber tension strength in direction 22, S_{f22T}, ksi	500
Fiber composite strength in direction 22, S_{f22c}, ksi	650
Fiber shear strength in direction 12, S_{f12s}, ksi	300
Fiber diameter, D_f, mils	5.6

(b) Ti-15-3-3-3 Matrix

Matrix density, ρ_m, lb/in.^{3}	0.172
Matrix elastic modulus, E_m, Mpsi	12.3
Matrix Poisson's ratio, υ_m, in./in.	0.32
Matrix shear modulus, G_m, Mpsi	4.7
Matrix coefficient of thermal expansion, α_m, ppm	4.5
Matrix melting temperture, T_{Mm}, °F	1800
Matrix tension strength, S_{mT}, ksi	130
Matrix composite strength, S_{mC}, ksi	130
Matrix shear strength, S_{mS}, ksi	91

(c) Composite

Composite density, ρ_c, lb/in.^{3}	0.147
Composite eleastic modulus in direction 11, E_{c11}, Mpsi	31.2
Composite elastic modulus in direction 22, E_{c22}, Mpsi	18.5
Composite elastic modulus in direction 33, E_{c33}, Mpsi	18.5
Composite shear modulus in direction 12, G_{c12}, Mpsi	7.7
Composite shear modulus in direction 23, G_{c23}, Mpsi	6.9
Composite shear modulus in direction 13, G_{c13}, Mpsi	7.7
Composite Poisson's ratio in direction 12, υ_{c12}, in./in.	0.31
Composite Poisson's ratio in direction 23, υ_{c23}, in./in.	0.33
Composite Poisson's ratio in direction 13, υ_{c13}, in./in.	0.31
Composite coefficient of thermal expansion in direction 11, α_{c11}, ppm	2.9
Composite coefficeint of thermal expansion in direction 22, α_{c22}, ppm	3.2
Composite coefficient of thermal expansion in direction 33, α_{c33}, ppm	3.2

TABLE II. - GRAPHITE P-100/COPPER ROOM TEMPERTURE MECHANICAL AND THERMAL PROPERTIES: COMPARISON OF METCAN PREDICTIONS AND THREE-DIMENSIONAL FINITE ELEMENT ANALYSIS

Property type	Fiber volume ratio							
	0.063		0.2234		0.466		0.622	
	METCAN	3-DFEM	METCAN	3-DFEM	METCAN	3-DFEM	METCAN	3-DFEM
$E_{\ell 11}$, mpsi	23.7	23.1	37.3	36.7	58.4	58.0	72.0	71.8
$E_{\ell 22}$, mpsi	13.8	14.9	10.2	11.0	6.5	6.9	4.6	5.0
$E_{\ell 33}$, mpsi	13.8	14.9	10.2	11.0	6.5	6.9	4.6	5.0
$G_{\ell 12}$, mpsi	5.8	6.0	4.5	4.8	3.2	3.4	2.5	2.6
$G_{\ell 23}$, mpsi	5.6	5.8	4.2	4.5	2.8	2.7	2.1	1.8
$G_{\ell 13}$, mpsi	5.8	5.8	4.5	4.5	3.2	2.7	2.5	1.8
$\upsilon_{\ell 12}$, in./in.	0.29	0.30	0.28	0.30	0.25	0.29	0.24	0.28
$\upsilon_{\ell 23}$, in./in.	0.30	0.30	0.30	0.26	0.30	0.22	0.30	0.19
$\upsilon_{\ell 13}$, in./in.	0.30	0.30	0.30	0.26	0.30	0.22	0.24	0.22
$\alpha_{\ell 11}$, ppm	6.8	6.6	3.3	3.7	1.0	1.40	0.18	0.42
$\alpha_{\ell 22}$, ppm	10.4	10.5	11.0	10.9	11.2	11.1	11.1	10.9
$\alpha_{\ell 33}$, ppm	10.4	10.5	11.0	10.9	11.2	11.1	11.1	10.9
$K_{\ell 11}$, Btu in./^{o}F hr in.^{2}	19.7	20.6	20.6	21.6	22.0	23.2	22.8	24.0
$K_{\ell 22}$, Btu in./^{o}F hr in.^{2}	15.6	17.3	11.8	13.5	7.8	8.8	5.8	6.3
$K_{\ell 23}$, Btu in./^{o}F hr in.^{2}	15.6	17.3	11.8	13.5	7.8	8.8	5.8	6.3

TABLE III. - HITCAN CAPABILITIES FOR COMPOSITE MATERIALS

Type of analysis	Type of structure				
	Beam	Plate	Ring	Curved panel	Builtup structure
Static	Tested	Tested	Tested	Tested	Tested
Buckling[a]					
Load stepping					
Modal (natural vibration modes)[b]					
Time domain	------	------	------	------	------
Loading:					
Mechanical	Tested	Tested	Tested	Tested	Tested
Thermal	Tested	Tested	Tested	Tested	Tested
Cyclic	------	------	------	------	------
Impact	------	------	------	------	------
Constitutive models[c]:					
P = constant	Tested	Tested	Tested	Tested	Tested
P = f(T) (temperture dependence)					
P = f(σ) (stress dependence)					
P = f($\dot{\sigma}$) (stress rate dependence)					
P = f(t) (creep)	------	------	------	------	------
P = f(T,σ,$\dot{\sigma}$) (combination)	Tested	Tested	Tested	Tested	Tested
P = f(T, σ,$\dot{\sigma}$,t) (creep combination)	------	------	------	------	------
Fiber Degradation	Tested	Tested	Tested	Tested	Tested
Fabrication induced stresses	Tested	Tested	Tested	Tested	Tested
Ply orientations[d] (arbitrary)	Tested	Tested	Tested	Tested	Tested

[a]Tested one buckling mode.
[b]Tested four vibration modes.
[c]Constitutive model notation: P, material properties; T, temperature; σ, stress; $\dot{\sigma}$, stress rate; t, time.
[d]Tested three ply orientations: unsymmetric (0/+45/90); symmetric $(0/45)_s$; balanced $(0/90)_s$.

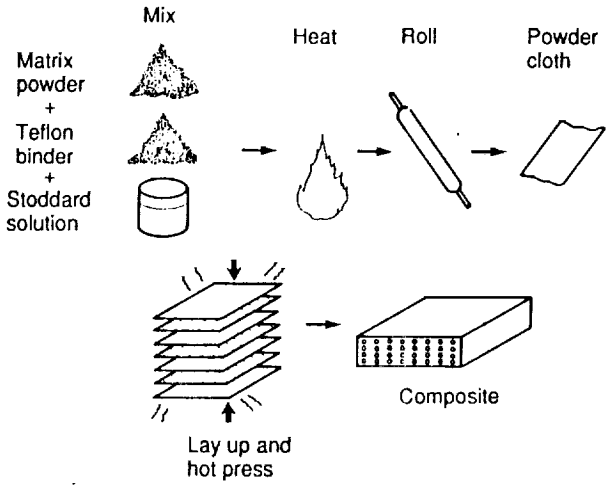

Figure 1.—Metal-matrix composite fabrication process.

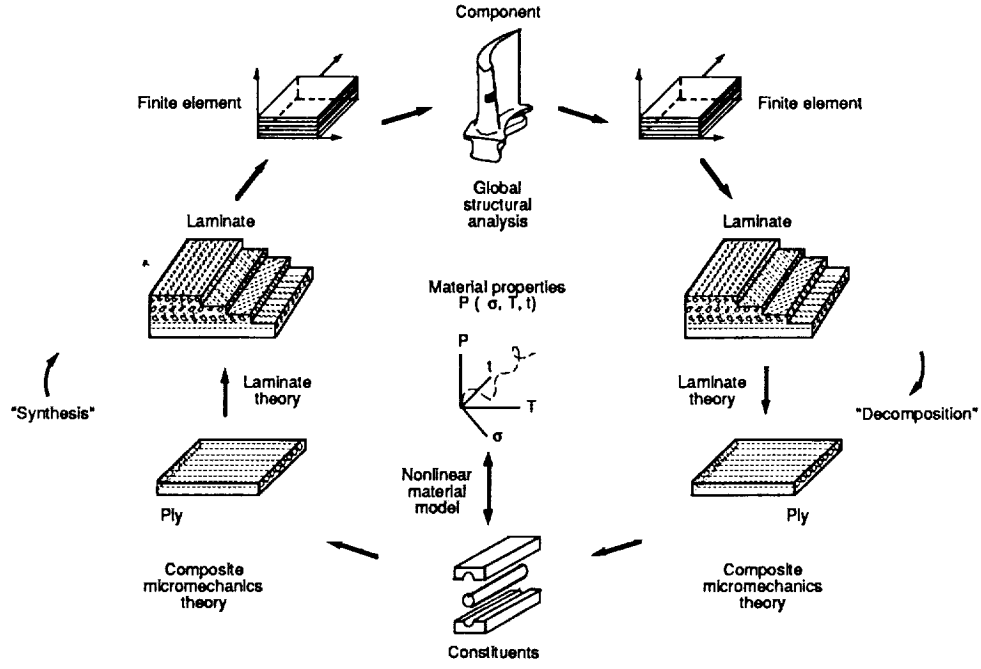

Figure 2.—Integrated approach to metal-matrix composite analysis.

$$\frac{P}{P_O} = \left[\frac{T_F - T}{T_F - T_O}\right]^n \left[\frac{S_F - \sigma}{S_F - \sigma_O}\right]^m \left[\frac{\dot{S}_F - \dot{\sigma}_O}{\dot{S}_F - \dot{\sigma}_O}\right]^l \left[\frac{\dot{T}_F - \dot{T}}{\dot{T}_F - \dot{T}_O}\right]^k \left[\frac{R_F - R}{R_F - R_O}\right]^p L$$

$$L \left[\frac{N_{MF} - N_M}{N_{MF} - N_{MO}}\right]^q \left[\frac{N_{TF} - N_R}{N_{TF} - N_{TO}}\right]^r \left[\frac{t_F - t}{t_F - t_O}\right]^s L$$

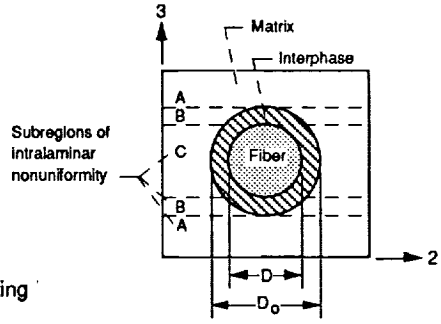

Rationale:

- Gradual effects during most range, rapidly degrading near final stages
- Representative of the in situ behavior for fiber, matrix, interphase, coating
- Introduction of primitive variables (PV)
- Consistent in situ representation of all constituent properties in terms of PV
- Room–temperature values for reference properties
- Continuous interphase growth
- Simultaneous interaction of all primitive variables
- Adaptability to new materials
- Amenable to verification inclusive of all properties
- Readily adaptable to incremental computational simulation

Notations:

P – property; T – temperature; S – strength; R – metallurgical reaction; N – number of cycles: t – time; over dot – rate; subscripts: O – reference; F – final; M – mechanical; T – thermal

Figure 3.—Assumed multifactor interaction relationship to represent the various factors which influence in situ constituent materials behavior.

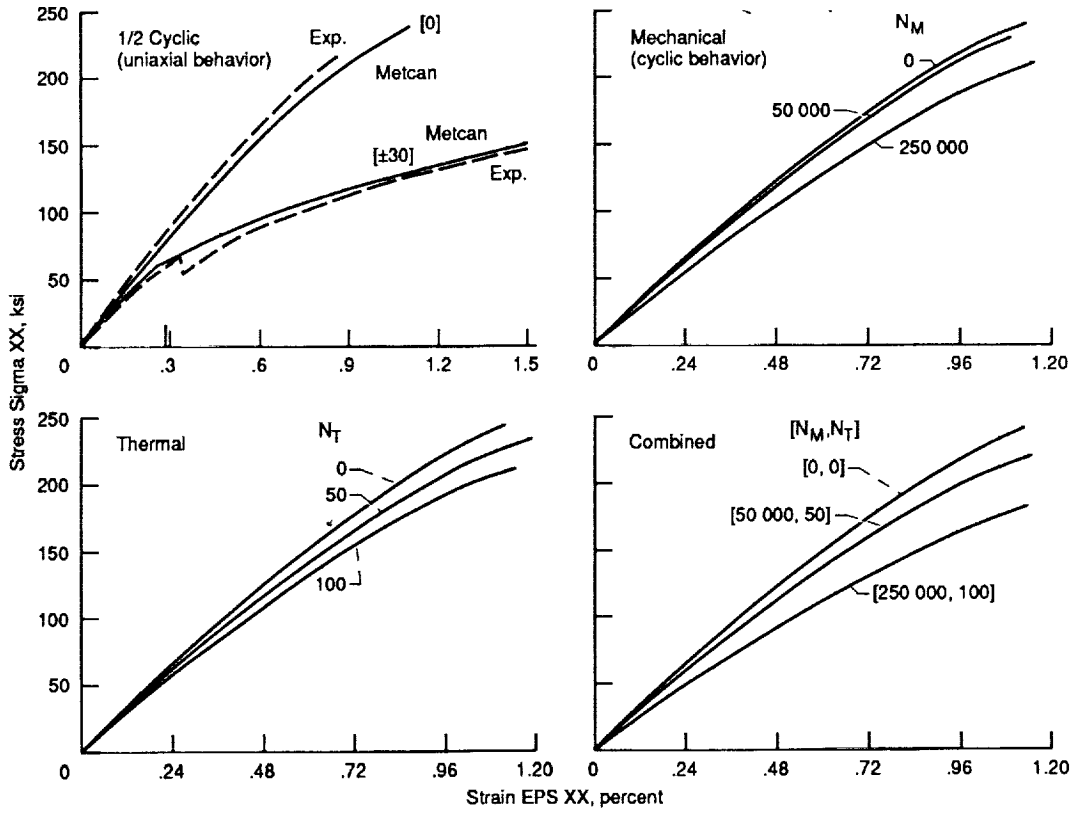

Figure 4.—Metcan predictions for thermomechanical cycling of MMC (SiC/Ti 15 333 at .36 FVR).

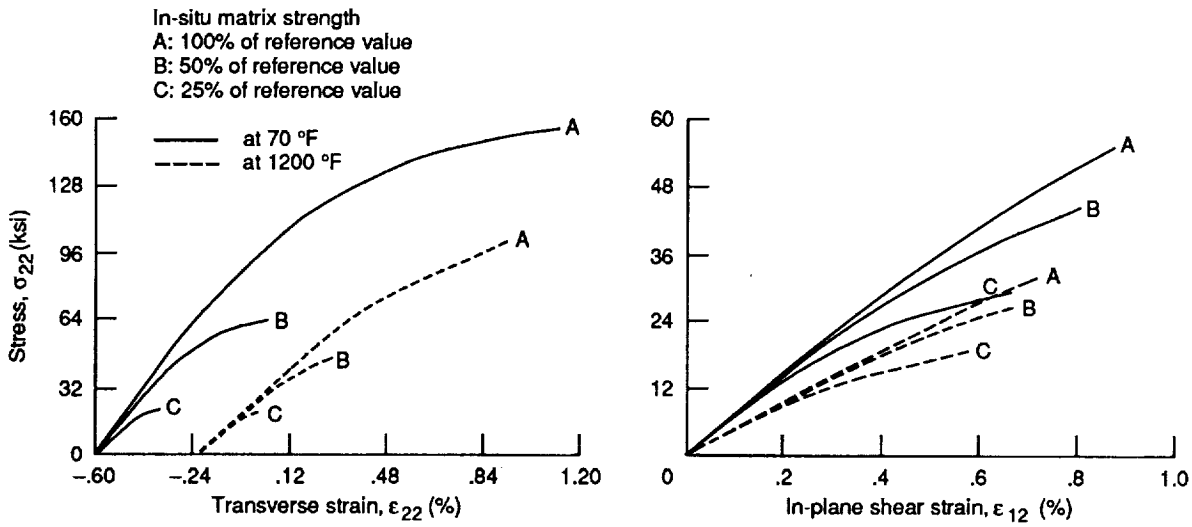

Figure 5.—Influence of in-situ matrix strength on the response of SiC/Ti-15-3-3-3 unidirectional composite.

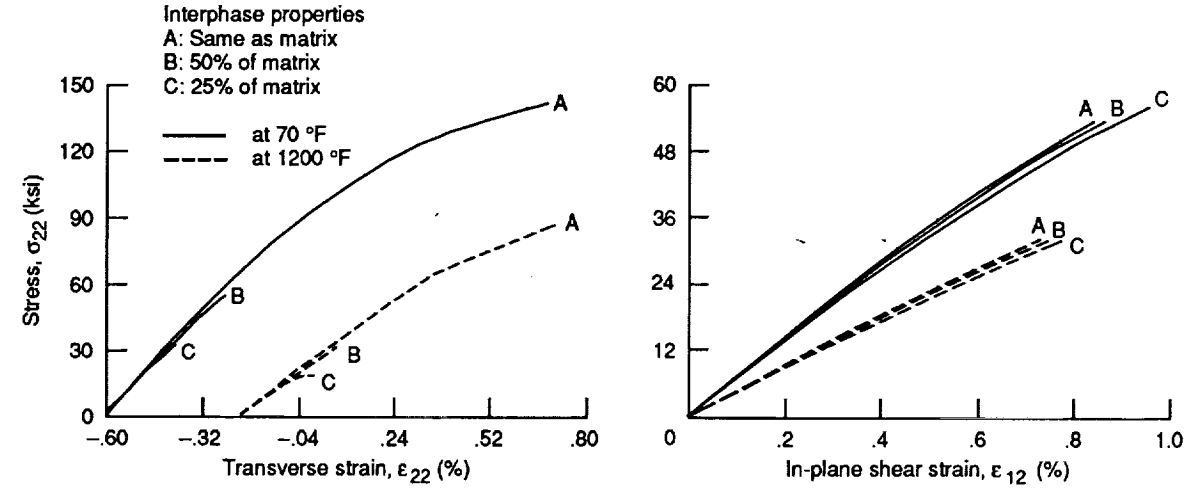

Figure 6.—Influence of interphase property degradation on the response of SiC/Ti-15-3-3-3 unidirectional composite.

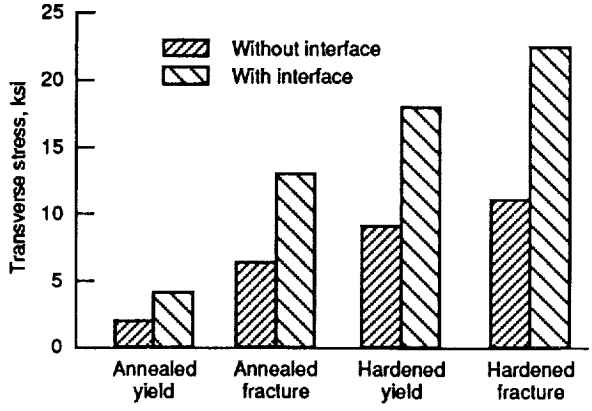

Figure 7.—Unidirectional graphite/copper MMC transverse strength bounds.

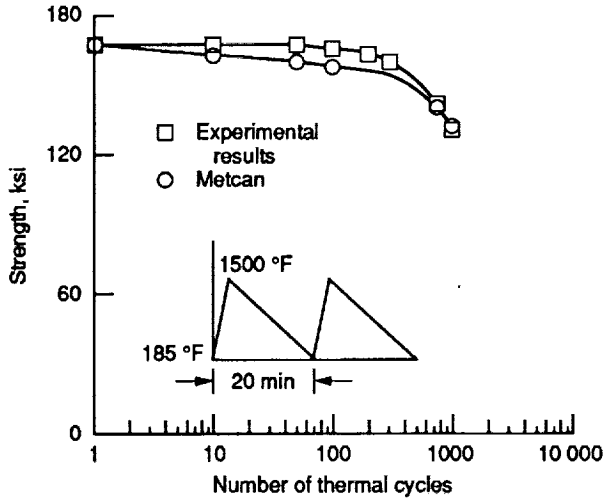

Figure 8.—Metcan simulates thermal fatigue strength of unidirectional SiC/Ti composite. (FVR .35; T = 70 °F).

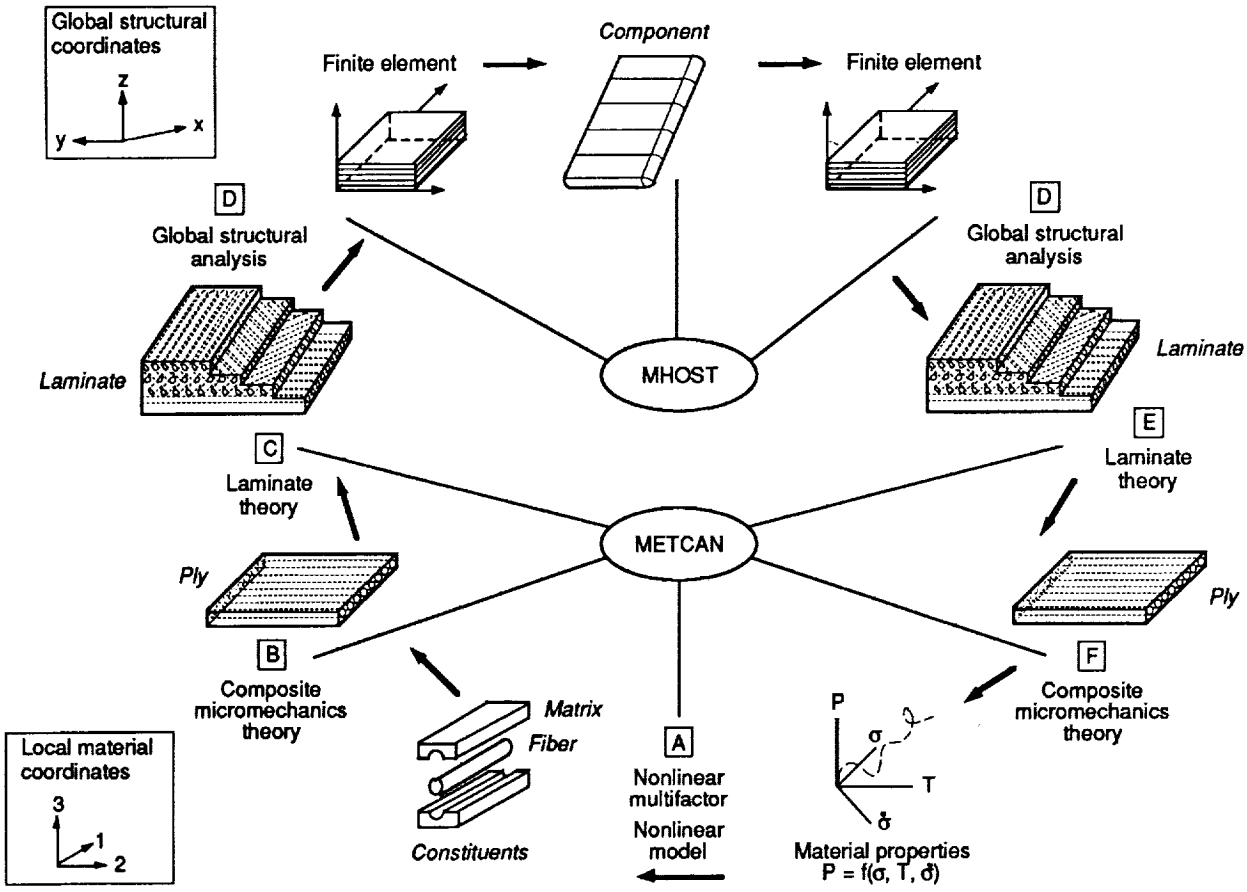

Figure 9.—HITCAN: An integrated computer code for high temperature composite structural analysis.

Fixed-free curved panel under bending and uniform temperature loadings for (SiC/Ti-15-3-3-3, 0/±45/90); 0.4 fiber volume ratio

Geometry

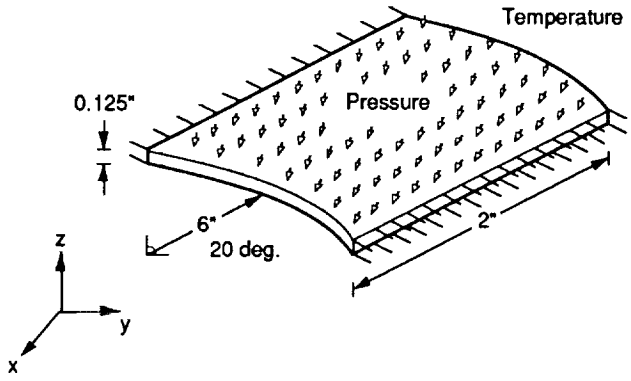

Loading

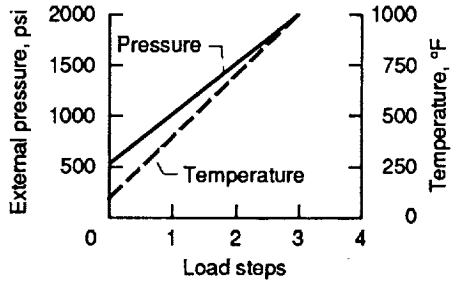

Figure 10.—Geometry and loading for curved panel.

Fixed-free curved panel under external pressure and uniform temperature loadings for (SiC/Ti-15-3-3-3, 0/±45/90); 0.4 fiber volume ratio

Geometry and loading

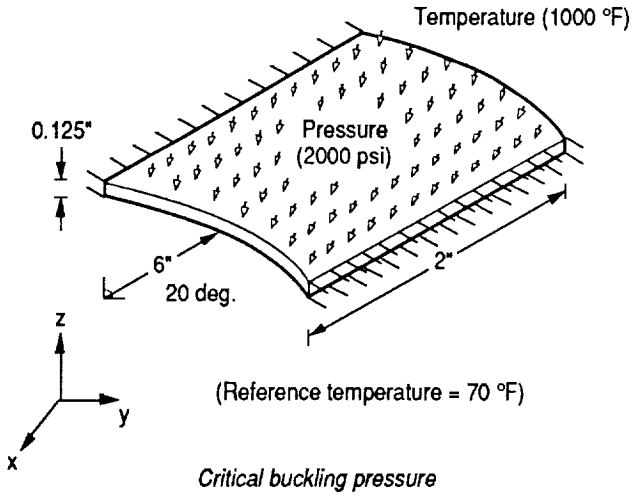

(Reference temperature = 70 °F)

Critical buckling pressure

(1) Under mechanical loading only = 38053 psi
(2) With fiber degradation, under mechanical loading only = 35437 psi
(3) Under thermo-mechanical loading = 25000 psi

Figure 11.—Buckling analysis for curved panel under thermo-mechanical loading.

Fixed-free curved panel under bending and uniform temperature loadings for (SiC/Ti-15-3-3-3, 0/±45/90); 0.4 fiber volume ratio

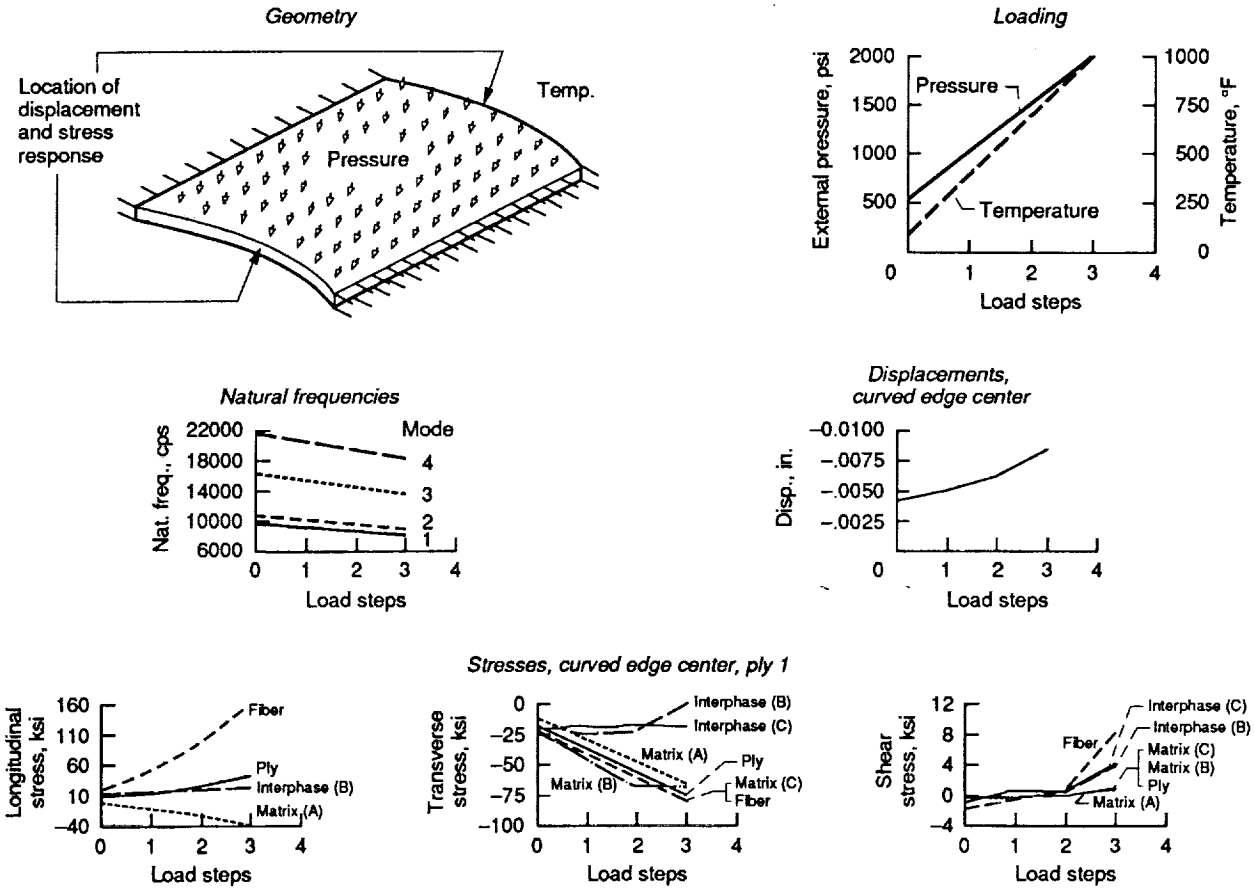

Figure 12.—Base case results for curved panel.

Fixed-free curved panel under bending and uniform temperature loadings for (SiC/Ti-15-3-3-3, 0/±45/90); 0.4 fiber volume ratio
Response: at load step 3

Geometry and loading

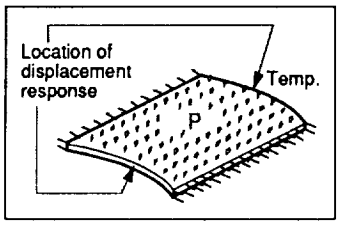

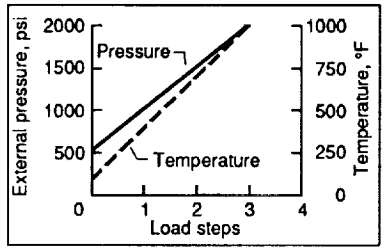

Fabrication-induced stresses

Fabrication-induced stresses	Disp. [free end center] (inch)	Stresses, ply 1 [fixed end center] (ksi)		
		Longitudinal	Transverse	Shear
No	–0.0157	40.9	–48.6	1.4
Yes	–0.0130	30.6	–47.4	0.5

Fiber degradation

Degradation	Disp. [free end center] (inch)	Stresses, ply 1 [fixed end center] (ksi)		
		Longitudinal	Transverse	Shear
No	–0.0157	40.9	–48.6	1.4
Yes	–0.0170	26.3	–36.9	1.1

Ply orientations

Orientation	Disp. [free end center] (inch)	Stresses, ply 1 [fixed end center] (ksi)		
		Longitudinal	Transverse	Shear
(0/±45/90)	–0.0157	40.9	–48.6	1.4
$(0/45)_s$	–0.0115	20.6	–48.4	0.3
$(0/90)_s$	–0.0115	18.4	–49.0	0.0

Constitutive relationships
(nonlinear multi-factor interaction model)

Relationship	Disp. [free end center] (inch)	Stresses, ply 1 [fixed end center] (ksi)		
		Longitudinal	Transverse	Shear
P = constant	–0.0135	36.4	–57.8	1.1
P = f(T) Temp. dependence	–0.0153	44.3	–54.9	1.3
P = f(σ) Stress dependence	–0.0138	34.6	–50.2	1.1
P = f(σ̇) Stress rate dependence	–0.0135	36.0	–57.8	1.1
P = f(T, σ, σ̇) Combination	–0.0157	40.9	–48.6	1.4

Notation:
P = Material property
σ = Stress
T = Temperature
σ̇ = Stress rate

Figure 13.—Sensitivity analysis.

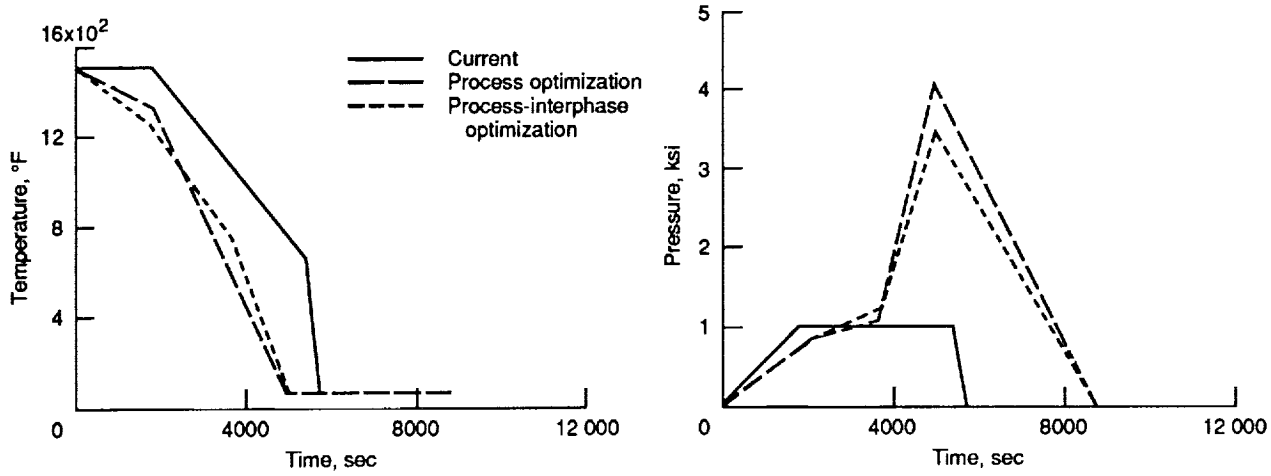

Figure 14.—Optimum and current cool-down phases for P100/copper.

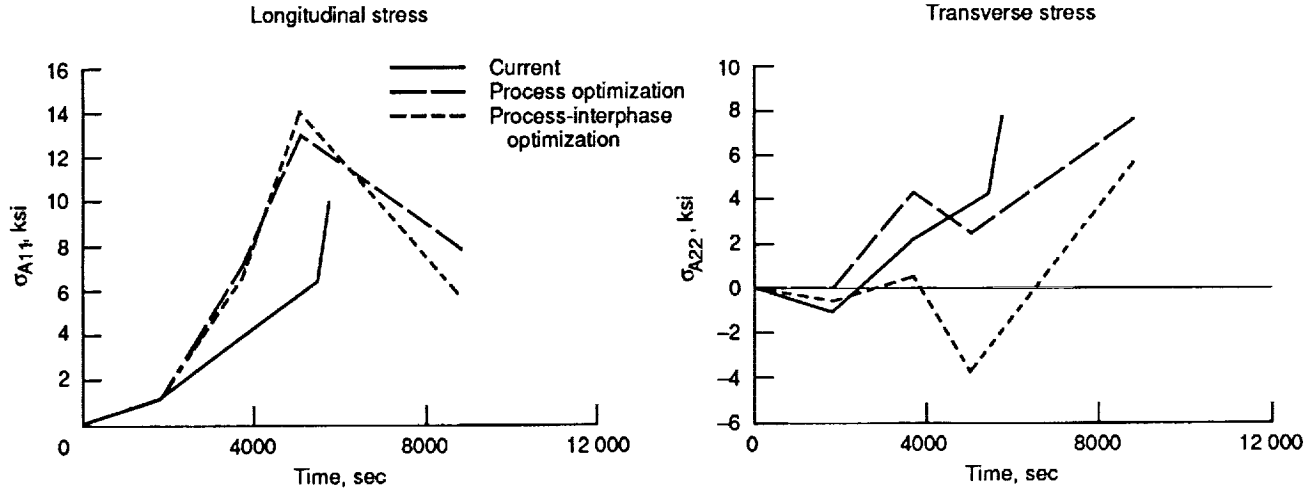

Figure 15.—Matrix microstresses developed during the cool-down phase of P100/copper.

NASA
National Aeronautics and Space Administration

Report Documentation Page

1. Report No.	2. Government Accession No.	3. Recipient's Catalog No.
NASA TM-103681		

4. Title and Subtitle	5. Report Date
Computational Simulation of Hot Composites Structures	6. Performing Organization Code

7. Author(s)	8. Performing Organization Report No.
C.C. Chamis, P.L.N. Murthy, and S.N. Singhal	E-5898
	10. Work Unit No. 510-01-0A

9. Performing Organization Name and Address	11. Contract or Grant No.
National Aeronautics and Space Administration Lewis Research Center Cleveland, Ohio 44135-3191	13. Type of Report and Period Covered Technical Memorandum
12. Sponsoring Agency Name and Address	14. Sponsoring Agency Code
National Aeronautics and Space Administration Washington, D.C. 20546-0001	

15. Supplementary Notes

Prepared for the Energy-Sources Technology Conference and Exhibition, sponsored by the American Society of Mechanical Engineers, Houston, Texas, January 20-24, 1991. Invited Paper. C.C. Chamis and P.L.N. Murthy, NASA Lewis Research Center. S.N. Singhal, Sverdrup Technology, Inc., Lewis Research Center Group, 2001 Aerospace Parkway, Brook Park, Ohio 44142.

16. Abstract

Three different computer codes developed in-house are described for application to hot composite structures. These codes include capabilities for: (1) laminate behavior (METCAN), (2) thermal/structural analysis of hot structures made from high temperature metal matrix composites (HITCAN), and (3) laminate tailoring (MMLT). Results for select sample cases are described to demonstrate the versatility as well as the application of these codes to specific situations. The sample case results show that METCAN can be used to simulate cyclic life in high temperature metal matrix composites; HITCAN can be used to evaluate the structural performance of curved panels as well as respective sensitivities of various nonlinearities; and MMLT can be used to tailor the fabrication process in order to reduce residual stresses in the matrix upon cool-down.

17. Key Words (Suggested by Author(s))	18. Distribution Statement
Metal matrix; SiC fibers; Graphite fibers; Titanium matrix; Copper matrix; Computer codes; Nonlinear behavior; Fabrication process; Curved panel; Finite element sensitivities tailoring; Cyclic life; Composite properties; In-situ strength	Unclassified – Unlimited Subject Category 24

19. Security Classif. (of this report)	20. Security Classif. (of this page)	21. No. of pages	22. Price*
Unclassified	Unclassified	18	A03

NASA FORM 1626 OCT 86

*For sale by the National Technical Information Service, Springfield, Virginia 22161